Available online at www.sciencedirect.com

ScienceDirect

www.elsevier.com/locate/jes

JES JOURNAL OF ENVIRONMENTAL SCIENCES

www.jesc.ac.cn

Structural characteristic and ammonium and manganese catalytic activity of two types of filter media in groundwater treatment

Ya Cheng, Tinglin Huang, Lijie Cheng, Yuankui Sun, Laisheng Zhu, Ye Li*

Key Laboratory of Northwest Resource, Environment and Ecology, MOE, Xi'an University of Architecture and Technology, Xi'an 710055, China
Shaanxi Key Laboratory of Environmental Engineering, Xi'an University of Architecture and Technology, Xi'an 710055, China

ARTICLE INFO

Article history:
Received 3 November 2017
Revised 22 December 2017
Accepted 22 December 2017
Available online 4 January 2018

Keywords:
Natural filter media
Active filter media
Manganese and ammonium removal
Manganese oxides
Characterization
Activity

ABSTRACT

Two types of filter media in groundwater treatment were conducted for a comparative study of surface structure and catalytic performance. Natural filter media was adopted from a conventional aeration–filtration groundwater treatment plant, and active filter media as a novel and promising filter media was also adopted. The physicochemical properties of these two kinds of filter media were characterized using numerous analytical techniques, such as X-Ray diffraction (XRD), scanning electron microscope (SEM), energy dispersive X-ray (EDX), X-ray photoelectron spectroscopy (XPS) and Zeta potential. The catalytic activities of these filter media were evaluated for ammonium and manganese oxidation. XRD data showed that both active filter media and natural filter media belonged to birnessite family. A new manganese dioxide (MnO_2) phase (PDF#72-1982) was found in the structure of natural filter media. The SEM micrograph of natural filter media showed honeycomb structures and the active filter media presented plate structures and consisted of stacked particle. These natural filter media presented lower level of some trace elements such as calcium and magnesium, lower degree of crystallinity, lower Mn(III) content and lattice oxygen content than that of active filter media, which were associated with its poor ammonium and manganese catalytic activities. In addition, some γ-Fe_2O_3 and $MnCO_3$ were found in the coating which may hinder the ammonium and manganese catalytic oxidation. This study provides a thorough and comprehensive understanding about the most commonly used filter media in water treatment, which can provide a theoretical guide to practical applications.

Introduction

Manganese (Mn^{2+}) and ammonium (NH_4^+) are common inorganic pollutants with salient features present in groundwater (Du et al., 2016; Tekerlekopoulou et al., 2013). Presence of manganese in finished water may cause organoleptic and operational problems including discoloration of water, unpleasant metallic taste and odor, increased turbidity and biofouling of pipelines as well as staining of laundry and plumbing fixtures (Cai et al., 2015; Hasan et al., 2013). The presence of ammonium in water systems also leads to oxygen depletion, eutrophication of surface water and toxicity for fish

* *Corresponding author. E-mail:* huangtinglin@xauat.edu.cn (Tinglin Huang).

https://doi.org/10.1016/j.jes.2017.12.014
1001-0742/

(Cai et al., 2015; Cheng et al., 2017a). The increasing and very often uncontrollable use of fertilizers has led to increased amounts of ammonium and manganese in potable water, which often exceed the upper permitted limit (Tekerlekopoulou and Vayenas, 2012). Most countries have their own maximum concentration limits as a guideline to produce good quality drinking water. The World Health Organization (WHO, 2004) has regulated that standard limits for NH_4^+–N and Mn^{2+} in drinking water should be below 1.5 and 0.1 mg/L, respectively (SEPA, 2002). In China, the maximum concentration limits for NH_4^+–N and Mn^{2+} in treated drinking water are 0.1 and 0.5 mg/L, respectively. Manganese and ammonium removal becomes a problem when using groundwater as a drinking water, especially in country sites, outside big cities (Taffarel and Rubio, 2010). Therefore, controlling the NH_4^+–N and Mn^{2+} content in drinking water has become a great public health issue.

Processes for the removal of ammonium ions from potable water include chlorination, ion exchange, membrane filtration and biological treatment processes (Oehmen et al., 2006; Vaaramaa and Lehto, 2003; Fu et al., 2011). Chlorination is usually limited due to the high volumes of sludge and the cost of the oxidants and ion exchange, and membrane filtration are limited due to their higher capital and operational costs (Tekerlekopoulou et al., 2013; Cai et al., 2015). Biological treatment processes as an additional and effective advanced biological system for the simultaneous removal of NH_4^+-N and Mn^{2+} in the treatment of drinking water attracts many attentions of researchers. However, actually numerous groundwater treatment facilities have opted to reduce their costs by applying origin quartz sand filter media without any pretreatment, which is called “conventional aeration-rapid sand filtration”. It is reported that more than 95% of the water treatment plants (WTPs) in China were still using the conventional water treatment process as of 2010 (Feng et al., 2012). Also, in European countries, the removal of manganese from groundwater is commonly achieved by aeration-rapids and filtration (Bruins et al., 2015a). The effect, over time, is the generation of a manganese oxide film on the media surface of the quartz sand (hereafter called the “natural filter media”). However, as general, in-rapid sand filters used for groundwater treatment, conditions for chemical formation of auto-catalytically active manganese oxides on virgin filter media, which can adsorb and subsequently oxidize dissolved manganese, are poor since most groundwater has a low redox potential and pH (Bruins et al., 2015a). Limited removal of manganese and ammonium could be achieved. Bruins et al. (2015a) have paid much excellent effort on how the filter media ripening process and confirmed the origin of the manganese oxide film. Some other researchers proposed the property of the manganese oxide depends on the valence of manganese in the oxide (Anschutz et al., 2005). Despite this, the relationship between the structure and ammonium and manganese catalytic activity of the mature filter media has not been established.

Besides, another novel and promising active manganese oxide filter media (hereafter called the “active filter media”) has been developed for simultaneous removal of ammonium and manganese in recent years and these filter media exhibit some advantages, such as short start-up time and good low temperature resistance (Guo et al., 2017; Cheng et al., 2017b, 2017c). This filter media have special ammonium and manganese catalytic oxidation ability (Cheng et al., 2017b). A review of water research publications was conducted in this research effort to seek out any previously performed studies related to the comparative investigation of structure and activity of these two types of filter media. However, up to now, rarely, work has been done on the comparative study of the above filter media.

In this study, we make a comparative study of the active filter media and natural filter media which have been running for more than one year. Structural (X-ray diffraction (XRD)), morphological (scanning electron microscope (SEM)), compositional (energy dispersive X-ray (EDX) spectroscopy) and elements state (X-ray photoelectron spectroscopy (XPS)) characterization of the filter film have been used to understand differences among these filter media and their effects on catalytic activity. Catalytic activity tests were carried out with contaminant such as ammonium and manganese.

1. Materials and methods

1.1. Source of filter media

The active filter media were adopted from pilot-scale water treatment plant. The initiating process of this type filter was carried out by oxidation–reduction method. The potassium permanganate ($KMnO_4$) solution, the manganese chloride ($MnCl_2$) solution and ferrous chloride ($FeCl_2$) solution were separately pumped into the tube. After mixed by static mixer, the oxidation reaction of manganese and iron with potassium permanganate are listed as follows:

$$3Fe^{2+} + MnO_4^- + 7H_2O \rightarrow 3Fe(OH)_3 + MnO_2 + 5H^+ \quad (1)$$

$$3Mn^{2+} + 2MnO_4^- + 2H_2O \rightarrow 5MnO_2 + 4H^+ \quad (2)$$

During the process, manganese and iron were dosed at the concentration of 2 and 1 mg/L, respectively. The concentration of potassium permanganate was determined by the stoichiometry, and then, iron-manganese oxides were generated. The iron-manganese oxides along with the raw water was carried to the filter and deposited on the surface of the quartz sands. With more and more iron-manganese oxides deposited during the initiating process, an active film finally was formed. The active filter has running continuously for 1 year. The active filter media samples were taken from the top of the filter bed.

The natural filter media were adopted from large water treatment plant. The characteristics of feed water are as follows: Fe 0.05–0.10 mg/L, Mn 0.05–0.10 mg/L, NH_4^+-N 0.01–0.10 mg/L, pH 7.8–8.0, Redox potential 200–280 mv and hardness190–200 mg/L. The feed water is faced with seasonal iron and manganese pollution and ammonium in the feed water is always below the limited concentration (<0.5 mg/L). This plant has been running for more than 1 year. A thick film was formed on the surface of the quartz sand. All filter media samples were taken from the top of the filter bed.

1.2. The operation of the filters

Two identical filters were adopted for the ammonium and manganese catalytic oxidation tests. Each filter consisted of a 200-cm-high Plexiglas column with an inside diameter of 10 cm. Natural filter media and active filter media were used as the filtration media, respectively. The filter bed was 120 cm high. Eight sampling points (located at 0, 20, 45, 60, 75, 90, 105, 120 cm from bottom to top) were attached along the height of the column. Groundwater pumped from a water source well was used as the feeding water. The concentration of dissolved oxygen (DO) in the influent was between 6.0 and 7.0 mg/L. The influent ammonium and manganese concentrations were kept at 1.5 and 2.0 mg/L, respectively.

1.3. Analytic methods

During all the experiments, samples were collected in 500-mL polypropylene bottles and immediately analyzed after sampling. NH_4^+, nitrite (NO_2^-), nitrate (NO_3^-) and Mn^{2+} were detected by spectrophotometry. Temperature (T), dissolved oxygen (DO) and pH were determined by a portable instrument (HACH, HQ30d, USA). Alkalinity was determined by acid–base titration.

1.4. Characterization

The structures of the samples were examined by XRD using Rigaku Ultiman IV with Cu Kα radiation (1.54 Å) at room temperature, which provided the structural investigation of the samples with data collected in the range of 5 to 75° at a scan rate of 5°/min. These experiments were operating at 40 kV and 40 mA and a step width of 0.02°. The morphology of the samples was observed using a field emission SEM (FEI Quanta 600F). EDX spectroscopy was performed to determine the chemical composition in the filter media samples using the same instrument with SEM with an Oxford INCA/ENERGY-350. XPS (K-Alpha XPS, Thermo Electron Corporation) was carried out to investigate the chemical oxidation states of elements Charging effects were corrected by adjusting the binding energy of C 1s to 284.6 eV. Zeta potential measurements were carried out with a Zetasizer Nano ZS90 (Malvern Instruments).

2. Results and discussion

2.1. Characterization of the filter media

2.1.1. Component analysis

EDX spectroscopy was used to investigate the surface element composition. As can be seen from Table 1, the major elements constituting the deposits on the filter media were manganese, iron, calcium, silicon, magnesium and oxygen. Manganese and iron contents accounted for a larger proportion of the deposits of active filter media (11.71% and 6.45%) than that of natural filter media (4.96% and 1.87%), which was called iron-manganese oxide film. Besides, it is important to note that a major difference between active filter media and natural filter media is that more calcium and magnesium was detected on the surface of active filter media than that on the surface of natural filter media.

Table 1 – Atomic ratios of the active filter media and natural filter media determined by energy dispersive X-ray (EDX).

Element	Si	O	Mg	Ca	Mn	Fe
Active filter media	15.58%	62.67%	1.05%	2.39%	11.71%	6.45%
Natural filter media	15.34%	76.19%	0.68%	0.95%	4.96%	1.87%

2.1.2. Surface morphology and Zeta potential behavior analysis

Significant difference in appearance can be seen with the naked eye, as can be seen from photographs shown in Fig. 1a and b. The active filter media appears black, in comparison with the red brown natural filter media which may attribute to the presence of a certain amount of ferric oxide (Fe_2O_3) on the surface of the natural filter media. It could be further verified by Fe 2p XPS analysis (in Section 2.1.4). Figure 1c and d shows the SEM of the active filter media and the natural filter media taken at 50000× magnification, respectively. The SEM micrograph of active filter media presents plate structures and consists of stacked particle. The SEM micrograph of natural filter media shows honeycomb structures. According to Bruins et al. (2015a), biologically produced birnessite has a fluffy plate structure in contrast to physico-chemically formed birnessite that has a more coral or sponge type structure. The morphological feature of filter media collected in our study was differing from them. The morphologies of manganese oxide were various in a natural environment and were closely related with its forming environment. In our study, we can't determine the origin of the iron-manganese oxide film according to the morphological feature.

Figure 2 shows the Zeta potential behavior of natural filter media and active filter media as a function of pH. The surface charge of the filter media becomes more negative when the medium pH is increased as a result of increased ratio OH^- to the H^+ bounds. When the pH ranged from 7.0 to 9.0, the Zeta potential absolute value of the natural filter media was slightly less than that of the active filter media, implying the surface charge of the active filter media was a little more negative during the water treatment process.

2.1.3. Structure analysis

XRD was used to identify phases and crystallinity of the oxide film samples (Fig. 3) (Kumar et al., 2015; Kuo et al., 2015). The XRD pattern obtained for active filter media samples compares well with previous studies, which have a mixed phase structure (birnessite, buserite PDF#86-1630). X-ray patterns of natural filter media samples also confirm to have a mixed phase structure (birnessite, buserite PDF#86-1630, MnO_2 PDF#72-1982). It has to be mentioned that the phase of silicon dioxide (SiO_2) (PDF#32-1128) are the experimental artifacts related to quartz sand, and thus, they should not be considered in the analysis of the filter film patterns. The big difference between active filter media samples and natural filter media samples was that a new MnO_2 phase (PDF#72-1982) was found in the structure of natural filter media samples. In addition, in comparison with active filter media, XRD patterns of natural filter media samples showed low peak intensities and peak broadening. This indicated low crystallinity of the natural filter media (Iyer et al., 2015). A comparison of XRD patterns in Fig. 3 showed

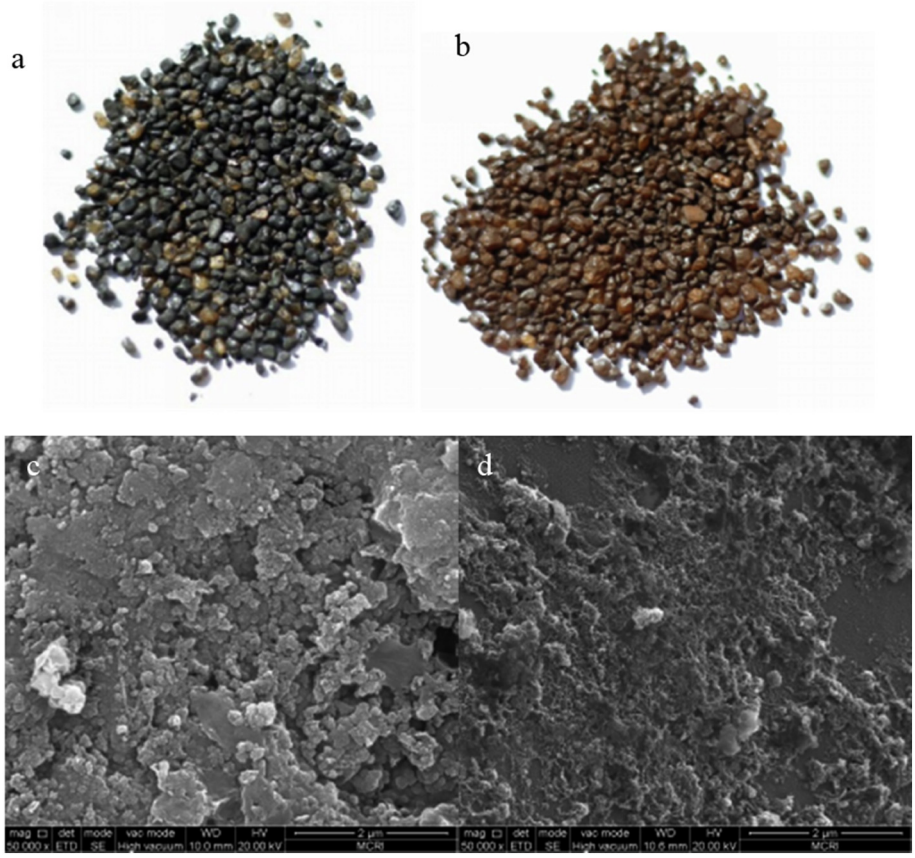

Fig. 1 – (a) Photographs of the active filter media, (b) photographs of the natural filter media, (c) scanning electron microscopy (SEM) of the active filter media (50000×), (d) surface of natural filter media (50000×).

that both of the filter media were belong to birnessite (Cheng et al., 2017b).

2.1.4. XPS analysis

XPS was conducted to identify surface manganese elemental binding energies (Zhang et al., 2012; Park, 2002). Both active filter media samples and natural filter media samples collected at the 3rd and 7th day were analyzed by XPS. As shown in Fig. 4, the high resolution XPS spectrum of Mn2p can be deconvoluted into three different components to reveal a characteristic of a mixed-valence manganese system. According to Batis et al. (2005), the peak positions of Mn2p3/2 level of MnO, Mn_2O_3 and MnO_2 were 640.6, 641.9 and 642.2 eV, respectively. The results indicate the presence of three manganese species, i.e., Mn(II), Mn(III) and Mn(IV), differently concentrated in the two types of filter media samples. According to XPS data, the

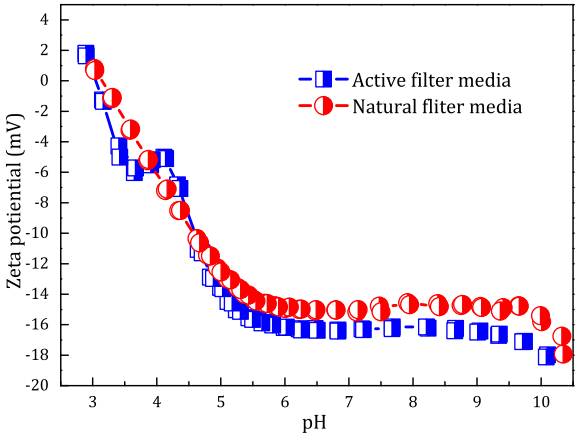

Fig. 2 – Zeta potential of the active filter media and the natural filter media as a function of pH.

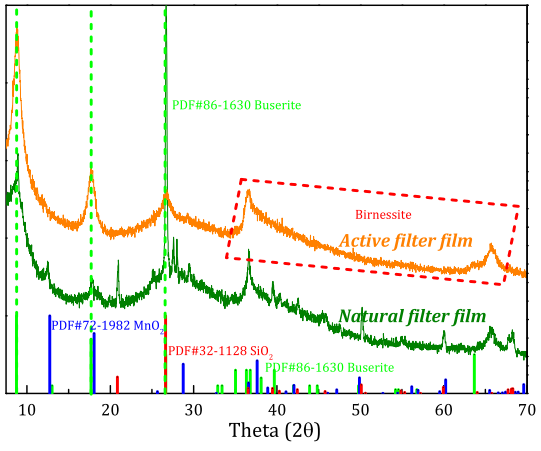

Fig. 3 – X-ray diffraction patterns of the active filter film and natural filter film.

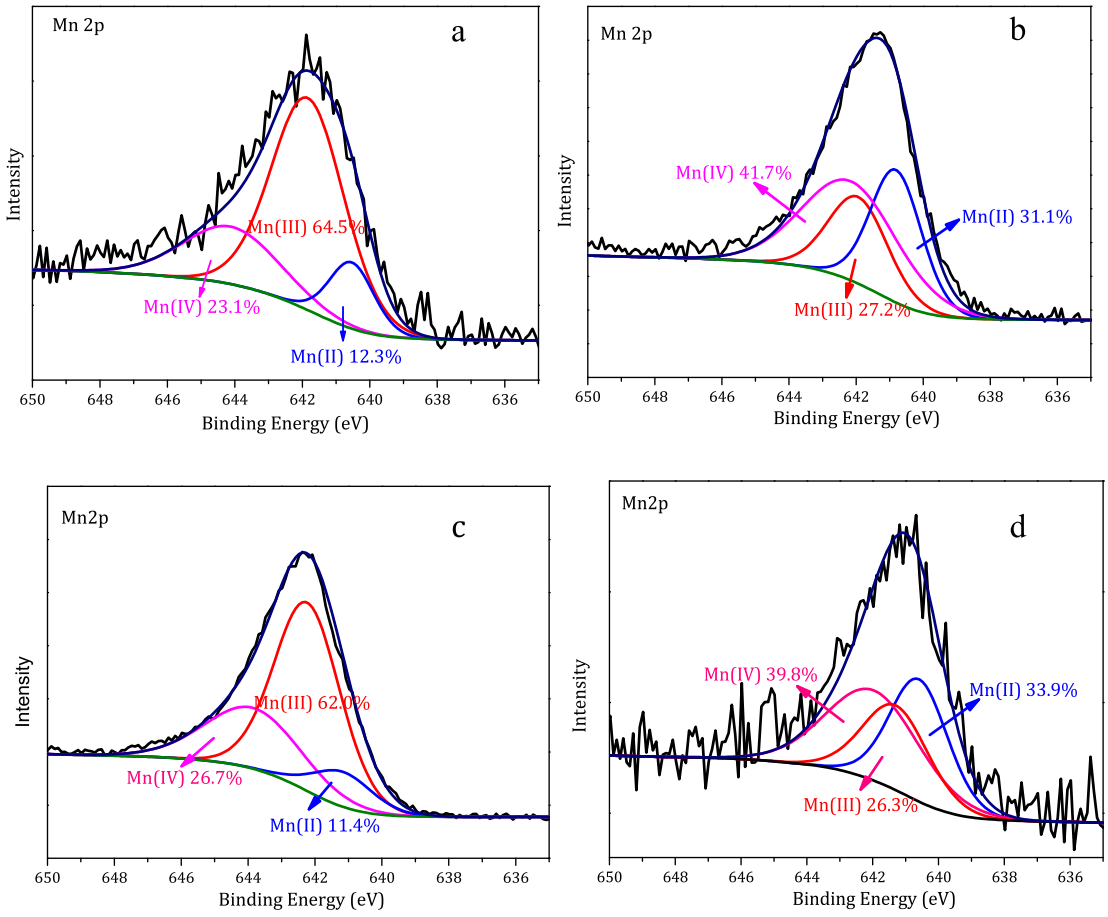

Fig. 4 – X-ray photoelectron spectroscopy (XPS) spectra of (a) Mn 2p3/2 of the active filter media collected at the 3rd day, (b) Mn 2p3/2 of the natural filter media collected at the 3rd day, (c) Mn 2p3/2 of the active filter media collected at the 7th day, (d) Mn 2p3/2 of the natural filter media collected at the 7th day.

Mn(II), Mn(III) and Mn(IV) atomic concentrations (%) in active filter media samples collected at the 3rd day (Fig. 4a) were 12.3%, 64.5% and 23.1%, whereas in the natural filter media samples collected at the 3rd day (Fig. 4b), they were 31.1%, 27.2%, and 41.7%, respectively, which indicate more Mn(III) were involved in active filter media samples. In addition, more Mn(IV) was involved in natural filter media samples which was in accordance with the XRD analysis. A new MnO_2 phase (PDF#72-1982) was found in the structure of natural filter media samples. In addition, it was found that the content of Mn(III) in both active filter media samples and natural filter media samples collected at the 7th day (Fig. 4c and d) varied slightly with that of the filter media samples collected at the 3rd day (Fig. 4a and b), which indicated that the content of Mn(III) in both active filter media samples and natural filter media samples remained unchanged during the water treatment.

Deconvolutions of the O1s XPS spectrum were also performed and are shown in Fig. 5. The O1s peak is attributed to O species derived from different oxygen sources. The spectrum can be deconvoluted into three components, which are related to lattice oxygen (528.9–529.2 eV), carbonates (530.9–531.4 eV), and hydroxyl groups or adsorbed O^- species (532.6–532.8 eV) (Batis et al., 2005). The results indicated that more carbonates were involved in natural filter media samples, and also it is noteworthy that more Mn(II) exist in these samples according to XPS Mn2p analysis. Therefore, we speculate the presence of larger amounts of manganese carbonate ($MnCO_3$) particles deposited on the filter media in the filter column. In addition, the XPS of the Ca2p level was also analyzed as shown in Fig. 6a. According to the literature, two doublets of the spectrum indicated the presence of calcium in different chemical surroundings and it might be due to the presence of calcium carbonate $CaCO_3$ (Batis et al., 2005; Zhang-Steenwinkel et al., 2002). The result was in accordance with the O1s spectrum where an additional peak was observed at BE of 530.9–531.4 eV. According to the redox-pH diagram of aqueous manganese (Fig. 6b) (Bruins et al., 2015a, 2015b; Stumm and Morgan, 1996), the pH and redox potential of feed water to the pilot (black dot) is in the transition zone of conditions for dissolved manganese and conditions theoretically required to form $MnCO_3$. This assumption was confirmed by the above analysis, where some $MnCO_3$ were found in the coating, especially in natural filter film. In addition, a higher lattice oxygen density was found in active filter media (Fig. 5a and c) than those in natural filter media (Fig. 5b and d). The content of lattice oxygen species in both active filter media samples and natural filter media samples collected at the 7th day

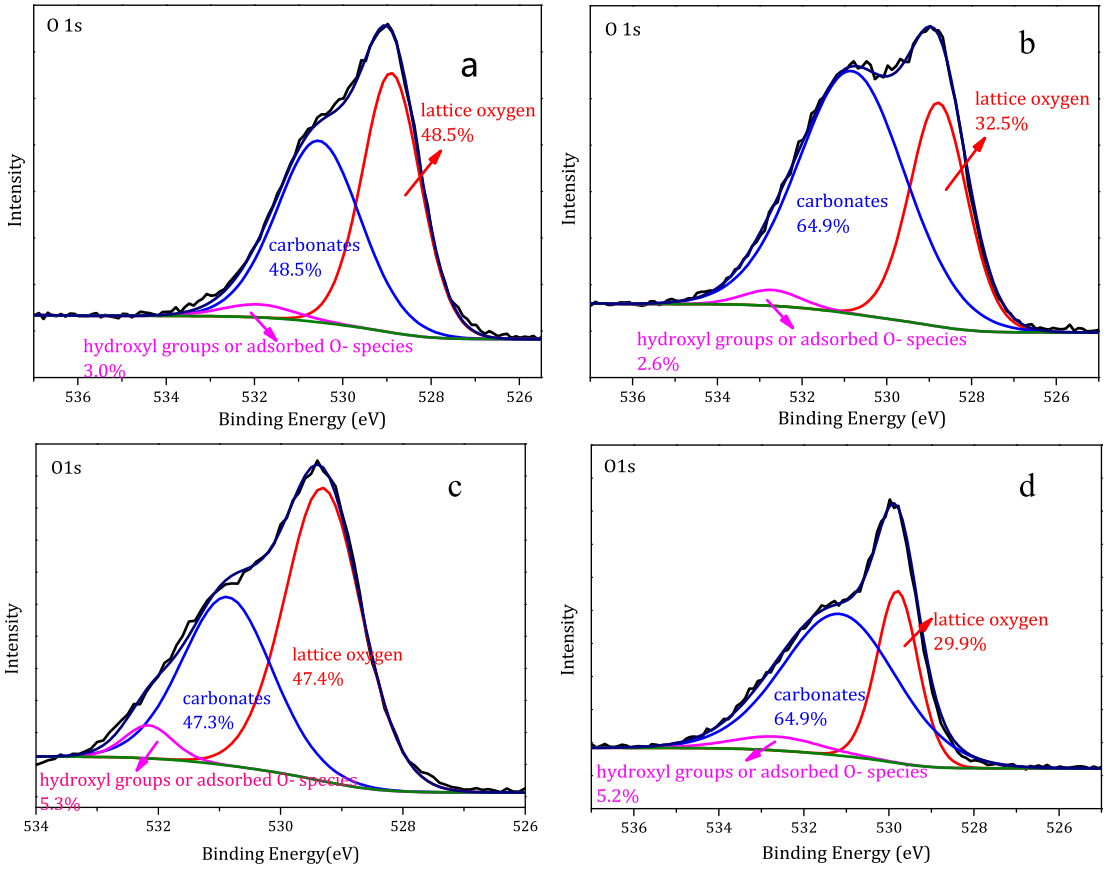

Fig. 5 – X-ray photoelectron spectroscopy (XPS) spectra of (a) O1s of the active filter media collected at the 3rd day, (b) O1s of the natural filter media collected at the 3rd day, (c) O1s of the active filter media collected at the 7th day, (d) O1s of the natural filter media collected at the 7th day.

(Fig. 5c and d) varied slightly with that of the filter media samples collected at the 3rd day (Fig. 5a and b), which indicated that the content of lattice oxygen species in both active filter media samples and natural filter media samples also remained unchanged during the water treatment.

Figure 7 presents the XPS spectra of Fe 2p core level. XPS has been known to be sensitive to Fe(II) and Fe(III). Above all things, the key characteristic which distinguishes γ-Fe_2O_3 from Fe_3O_4 is the presence of the satellite peak at a binding energy of 719.0 eV (Sang et al., 2014; Gota et al., 1999). In our

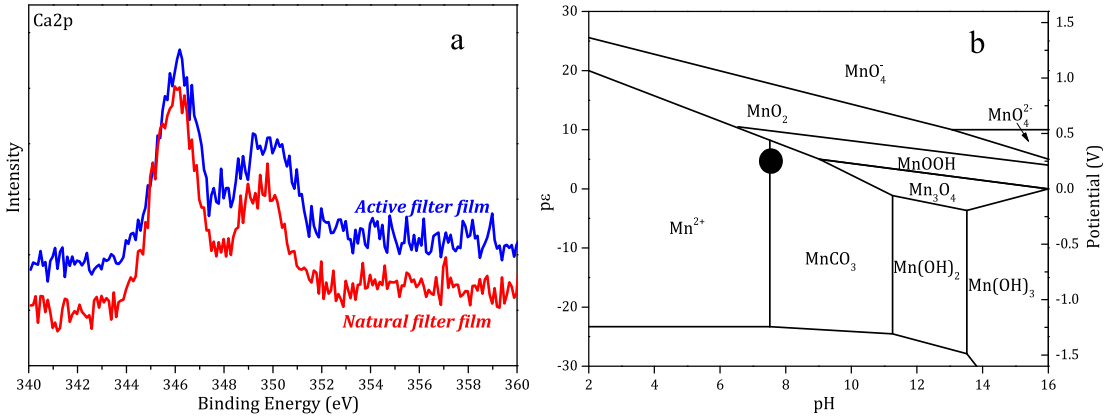

Fig. 6 – (a) XPS spectra of Ca 2p core level attained from active filter media and natural filter media collected at the 3rd day. (b) Electron activity (pε) or redox potential (Eh in e V) -pH diagram for aqueous manganese (adopted from Stumm and Morgan, 1996), compared to feed water conditions of the groundwater of the GWTPs (black dot).

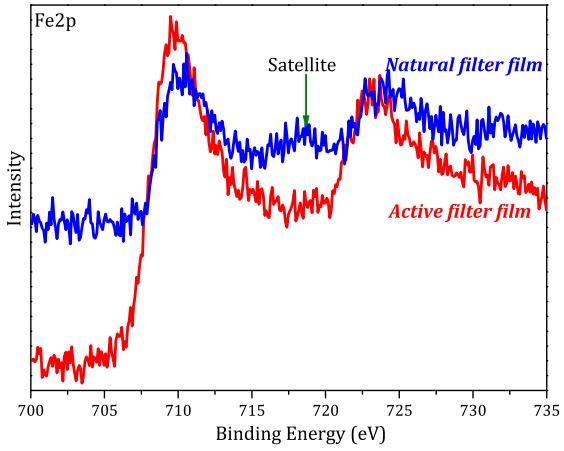

Fig. 7 – XPS spectra of Fe 2p core level attained from active filter media and natural filter media collected at the 3rd day.

case, the satellite peak was observable at a binding energy of 719.2 eV as indicated with an arrow in Fig. 7. Therefore, it is certain that non-negligible amount of γ-Fe_2O_3 were found in the natural filter film, which was closely related to the red brown layer coated on the surface of filter media (Fig. 1b).

2.2. Activity of the filter media

These two filters have operated for 7 days. Performance in terms of ammonium and manganese removal was systematically studied, and comparisons between this active filter media and natural filter media were carried out.

Figure 8 shows the performance of the natural filter and active filter with respect to simultaneous removal of NH_4^+-N and Mn^{2+} during the operation period. There was little difference (0.1–0.2 mg/L) between the influent and effluent Mn^{2+} concentration in the natural filter (as shown in Fig. 8b), indicating the limited manganese removal ability of the natural filter media. Similarly, the NH_4^+-N removal performance was poor (as shown in Fig. 8a). Unlike it, the filter filled with the active filter media demonstrated better ammonium and manganese removal ability (Fig. 8a and b). The effluent NH_4^+-N and Mn^{2+} could hardly be detected. Ammonium evolution in the filter system was confirmed by analyses of NO_3^- and NO_2^- in the solution. As illustrated in Fig. 8a, the decrease in NH_4^+-N concentration was accompanied with an elevation of NO_3^-, NO_2^- formation and DO consumption in active filter which was consistent with our previous study (Cheng et al., 2017b, 2017c). In contrast, the concentration of NO_3^-, NO_2^- and DO along the height of the natural filter column remained almost constant (data not shown).

In addition, the evolution of NH_4^+-N and Mn^{2+} along the height of these two filters was also determined. As can be seen from Fig. 9, the relative constant NH_4^+-N and Mn^{2+} concentration along the height of the pilot column filled with the natural filter media further confirmed that under the adopted reaction conditions there was no occurrence of NH_4^+-N and Mn^{2+} catalytic reaction. In contrast, the NH_4^+-N and Mn^{2+} concentration decreased along the height of the active filter, and at a depth of 60 cm (total 120 cm), NH_4^+-N could go below the maximum concentration limits (<0.5 mg/L) (Fig. 9a), and almost all Mn^{2+} could have been removed (Fig. 9b). Obviously, natural filter media was less active than active filter media for NH_4^+-N and Mn^{2+} catalytic oxidation.

2.3. The relationship between structure and activity

In the aqueous system, the metal oxides have surface hydroxyl groups that have acidic and basic characteristics (Taffarel and Rubio, 2010). According to the analysis of Zeta potential, the surface charge of the active filter media was just a little more negative than that of the natural filter media during the water treatment process. Even so, the little difference in the surface charge couldn't determine the ammonium and manganese removal performance. Therefore, we speculate the difference between the two types of the filter media in ammonium and manganese catalytic activity did not arise from the difference of the surface hydroxyl groups.

It is well known that the catalytic activity of iron-manganese oxide is associated with its composition and structure. As

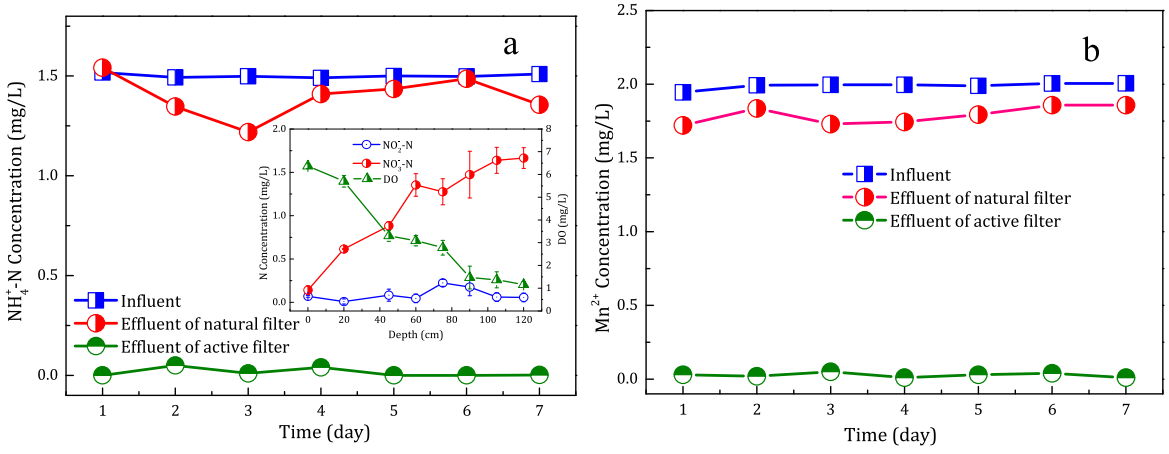

Fig. 8 – The running performance of the natural filter and active filter with respect to simultaneous removal of ammonium (NH_4^+-N) (a) and manganese (Mn^{2+}) (b). The inset shows the profiles about the concentrations of nitrite (NO_2^--N), nitrate (NO_3^--N) and dissolved oxygen (DO), respectively, along the height of the active filter.

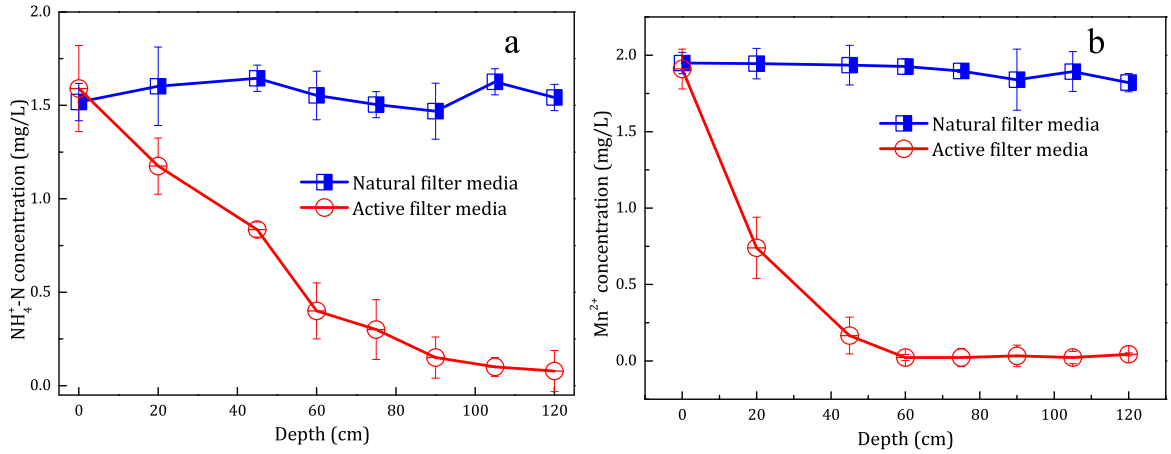

Fig. 9 – Concentration profiles of ammonium (NH_4^+-N) (a) and manganese (Mn^{2+}) (b) along the height of the pilot column filled with the natural filter media and the active filter media.

revealed by the XPS investigation, more Mn(III) were involved in active filter media. Our previous research has shown that the highly catalytic activity of active birnessite involved in ammonium catalytic oxidation was proposed to be intermediated by Mn(III) (Cheng et al., 2017b). In addition, Peluso et al. (2008) studied the manganese dioxide catalyzed oxidation of ethanol, and suggested that a high concentration of Mn(III) could result in weak Mn – O bonds, which might ensure good catalytic activity. XRD data showed that both active filter media and natural filter media belonged to the birnessite family. The difference of phase constitution and crystallinity helped to explain the ammonium and manganese catalytic activity differences between them. Compared with the active filter media, a new MnO_2 phase (PDF#72-1982) was found in the structure of natural filter media. Mn(IV) phase was less active than Mn(III) phase. What's more, a higher lattice oxygen density was found in active filter media. According to the literature, structural defect is beneficial for the activation of oxygen molecules to active oxygen adspecies (Wang et al., 2012). Specifically, lattice oxygen species with high mobility enhanced the formation of surface active oxygen species through the complex migration between surface lattice oxygen and oxygen vacancy with molecular oxygen (Zhu et al., 2017). Therefore, the Mn(III) content and the oxygen adspecies concentration relevant to the surface oxygen vacancy density were correlative with the catalytic activity of these filter media samples. In addition, the content of Mn(III) and concentration of lattice oxygen species in both active filter media samples and natural filter media samples remained almost unchanged during the water treatment, which suggested that there was no loss of the active components. It was in accordance with the stable removal efficiency of ammonium and manganese during the operation period (Fig. 8).

Another major difference between active filter media and natural filter media was that more calcium and magnesium was detected on the surface of active filter media. A survey of the literature available showed that heteroatom doping in the manganese oxides can also improve catalytic activities to some extent, which is ascribed to the generated defects or synergistic effects (Wang et al., 2017). In addition, Wang et al. (2015, 2017) reported that the content of water and interlayer cations in birnessite had dramatic effect on its activity due to their influence on surface hydroxyl, which acted as active species in formaldehyde oxidation. Some γ-Fe_2O_3 and $MnCO_3$ were found in the coating, especially in natural filter media. According to Bruins et al. (2015a), $MnCO_3$ has no auto-catalytical adsorption and oxidation properties, which consequently hindered the ammonium and manganese catalytic oxidation.

Therefore, we concluded that the poor catalytic performance of natural filter media was mainly related to the low Mn(III) content, the lattice oxygen and heteroatom doping. In addition, the presence of $MnCO_3$ may hinder the ammonium and manganese catalytic oxidation.

3. Conclusion

The following conclusions can be drawn based on the results emerging from this study: (1) Analysis of XRD data showed that both active filter media and natural filter media belong to the birnessite family. A new MnO_2 phase (PDF#72-1982) was found in the structure of natural filter media samples. (2) The morphological feature of active filter media was differing from natural filter media. The SEM micrograph of active filter media presented plate structures and consisted of stacked particle, and the natural filter media showed honeycomb structures. (3) Natural filter media was less active than active filter media for ammonium and manganese catalytic oxidation. (4) More Mn(III) and a higher lattice oxygen density were found in active filter media, and some γ-Fe_2O_3 and $MnCO_3$ were found in the coating of natural filter media, which was correlative with the catalytic activity of these filter media samples.

Acknowledgments

This work was supported by the National Key Research and Development Program of China (No. 2016YFC00400706), the National Natural Science Foundation of China (No. 51778521)

and the Natural Science Basic Research Plan in Shaanxi Province of China (No. 2017JQ2014).

REFERENCES

Anschutz, P., Dedieu, K., Desmazes, F., Chaillou, G., 2005. Speciation, oxidation state, and reactivity of particulate manganese in marine sediments. Chem. Geol. 218 (3), 265–279.

Batis, N.H., Delichere, P., Batis, H., 2005. Physicochemical and catalytic properties in methane combustion of $La_{1-x}Ca_xMnO_{3\pm y}$ ($0 \le x \le 1$; $-0.04 \le y \le 0.24$) perovskite-type oxide. Appl. Catal. A Gen. 282 (1), 173–180.

Bruins, J.H., Petrusevski, B., Slokar, Y.M., Huysman, K., Joris, K., Kruithof, J.C., Kennedy, M.D., 2015a. Biological and physico-chemical formation of birnessite during the ripening of manganese removal filters. Water Res. 69 (7053), 154.

Bruins, J.H., Petrusevski, B., Slokar, Y.M., Kruithof, J.C., Kennedy, M.D., 2015b. Manganese removal from groundwater: characterization of filter media coating. Desalin. Water Treat. 55 (7), 1–13.

Cai, Y., Li, D., Liang, Y., Luo, Y., Zeng, H., Zhang, J., 2015. Effective start-up biofiltration method for Fe, Mn, and ammonia removal and bacterial community analysis. Bioresour. Technol. 176 (16), 149–155.

Cheng, Y., Huang, T., Shi, X., Wen, G., Sun, Y., 2017a. Removal of ammonium ion from water by Na-rich birnessite: performance and mechanisms. J. Environ. Sci. 57 (7), 402–410.

Cheng, Y., Huang, T., Sun, Y., Shi, X., 2017b. Catalytic oxidation removal of ammonium from groundwater by manganese oxides filter: performance and mechanisms. Chem. Eng. J. 322 (15), 82–89.

Cheng, Y., Li, Y., Huang, T., Sun, Y., Shi, X., Shao, Y., 2017c. A comparison study of the start-up of a MnO_x filter for catalytic oxidative removal of ammonium from groundwater and surface water. J. Environ. Sci. https://doi.org/10.1016/j.jes.2017.07.008.

Du, X., Liu, G., Qu, F., Li, K., Shao, S., Li, G., Liang, H., 2016. Removal of iron, manganese and ammonia from groundwater using a PAC-MBR system: the anti-pollution ability, microbial population and membrane fouling. Desalination 403, 97–106.

Feng, S., Xie, S., Zhang, X., Yang, Z., Ding, W., Liao, X., et al., 2012. Ammonium removal pathways and microbial community in GAC-sand dual media filter in drinking water treatment. J. Environ. Sci. 24 (9), 1587.

Fu, J.X., Shang, J., Zhao, Y.H., 2011. Simultaneous removal of iron, manganese and ammonia from groundwater in single biofilter layer using baf. Adv. Mater. Res. 183-185, 442–446.

Gota, S., Guiot, E., Henriot, M., Gautier-Soyer, M., 1999. Atomic-oxygen-assisted MBE growth of $\alpha-Fe_2O_3$ on $\alpha-Al_2O_3$ (0001): metastable FeO(111)-like phase at subnanometer thicknesses. Phys. Rev. B 60 (20), 14387–14395.

Guo, Y., Huang, T., Wen, G., Cao, X., 2017. The simultaneous removal of ammonium and manganese from groundwater by iron-manganese co-oxide filter film: the role of chemical catalytic oxidation for ammonium removal. Chem. Eng. J. 308, 322–329.

Hasan, H.A., Abdullah, S.R.S., Kamarudin, S.K., Kofli, N.T., 2013. On–off control of aeration time in the simultaneous removal of ammonia and manganese using a biological aerated filter system. Process. Saf. Environ. Prot. 91 (5), 415–422.

Iyer, A., Delpilar, J., King'Ondu, C.K., Kissel, E., Garces, H.F., Huang, H., et al., 2015. Water oxidation catalysis using amorphous manganese oxides, octahedral molecular sieves (OMS-2), and octahedral layered (OL-1) manganese oxide structures. J. Phys. Chem. C 116 (10), 6474–6483.

Kumar, R.V., Ghoshal, A.K., Pugazhenthi, G., 2015. Fabrication of zirconia composite membrane by *in-situ* hydrothermal technique and its application in separation of methyl orange. Ecotoxicol. Environ. Saf. 121 (12), 73–79.

Kuo, C.H., Mosa, I.M., Poyraz, A.S., Biswas, S., El-Sawy, A.M., Song, W., et al., 2015. Robust mesoporous manganese oxide catalysts for water oxidation. ACS Catal. 5 (3), 1693–1699.

Oehmen, A., Viegas, R., Velizarov, S., Reis, M.A.M., Crespo, J.G., 2006. Removal of heavy metals from drinking water supplies through the ion exchange membrane bioreactor. Desalination 199 (1–3), 405–407.

Park, H.J., 2002. Interfacial properties of thin film hetero-structure: copper-oxides of hafnium-silicon. Diss. Abstr. Int. 64 (03), 1445.

Peluso, M.A., Gambaro, L.A., Pronsato, E., Gazzoli, D., Thomas, H.J., Sambeth, J.E., 2008. Synthesis and catalytic activity of manganese dioxide (type OMS-2) for the abatement of oxygenated VOCs. Catal. Today 133–135 (1), 487–492.

Sang, Y.L., Kim, D.H., Choi, S.C., Lee, D.J., Ji, Y.C., Kim, H.D., 2014. Porous multi-walled carbon nanotubes by using catalytic oxidation via transition metal oxide. Microporous Mesoporous Mater. 194 (4), 46–51.

SEPA (State Environmental Protection Administration), 2002. Monitoring and Analytical Methods for Water and Wastewater. fourth ed. China Environmental Science Press, Beijing (in Chinese).

Stumm, W., Morgan, J.J., 1996. Aquatic Chemistry: Chemical Equilibria and Rates in Naturalwaters. Cram101 Textbook Outlines to Accompany 179 (11) p. A277.

Taffarel, S.R., Rubio, J., 2010. Removal of Mn^{2+} from aqueous solution by manganese oxide coated zeolite. Miner. Eng. 23 (14), 1131–1138.

Tekerlekopoulou, A.G., Vayenas, D.V., 2012. Ammonia, iron and manganese removal from potable water using trickling filters. Desalination 210 (1), 225–235.

Tekerlekopoulou, A.G., Pavlou, S., Vayenas, D.V., 2013. Removal of ammonium, iron and manganese from potable water in biofiltration units: a review. J. Chem. Technol. Biotechnol. 88 (5), 751–773.

Vaaramaa, K., Lehto, J., 2003. Removal of metals and anions from drinking water by ion exchange. Desalination 155 (2), 157–170.

Wang, F., Dai, H., Deng, J., Bai, G., Ji, K., Liu, Y., 2012. Manganese oxides with rod-, wire-, tube-, and flower-like morphologies: highly effective catalysts for the removal of toluene. Environ. Sci. Technol. 46 (7), 4034–4041.

Wang, J., Zhang, P., Li, J., Jiang, C., Yunus, R., Kim, J., 2015. Room-temperature oxidation of formaldehyde by layered manganese oxide: effect of water. Environ. Sci. Technol. 49 (20), 12372.

Wang, J., Li, J., Jiang, C., Zhou, P., Zhang, P., Yu, J., 2017. The effect of manganese vacancy in birnessite-type MnO_2 on room-temperature oxidation of formaldehyde in air. Appl. Catal. B Environ. 204, 147–155.

WHO, 2004. Guideline for Drinking Water Quality. third ed. vol. 1. World Health Organization, Geneva.

Zhang, T., Yan, X., Sun, D.D., 2012. Hierarchically multifunctional K-OMS-2/TiO_2/Fe_3O_4 heterojunctions for the photocatalytic oxidation of humic acid under solar light irradiation. J. Hazard. Mater. 243 (4), 302–310.

Zhang-Steenwinkel, Y., Beckers, J., Bliek, A., 2002. Surface properties and catalytic performance in CO oxidation of cerium substituted lanthanum–manganese oxides. Appl. Catal. A Gen. 235 (1–2), 79–92.

Zhu, L., Wang, J., Rong, S., Wang, H., Zhang, P., 2017. Cerium modified birnessite-type MnO_2 for gaseous formaldehyde oxidation at low temperature. Appl. Catal. B Environ. 211 (15), 212–221.